UNSUPERVISED SEGMENTATION FOR AUTOMATIC DETECTION OF BRAIN TUMORS IN MRI

A.S. Capelle, O. Alata, C. Fernandez, S. Lefevre

IRCOM-SIC, UMR-CNRS 6615
Univ. Poitiers, Bât. SP2MI
86962 Futuroscope Chasseneuil Cedex, FRANCE
capelle@sic.sp2mi.univ-poitiers.fr

J.C Ferrie

Dept. d'Imagerie Médicale
Unité IRM, SCANNER
BP 577 - 86021 Poitiers, FRANCE

ABSTRACT

In this paper, we present a new automatic segmentation method for magnetic resonance images. The aim of this segmentation is to divide the brain into homogeneous regions and to detect the presence of tumors. Our method is divided into two parts. First, we make a pre-segmentation to extract the brain from the head. Then, a second segmentation is done inside the brain. Several techniques are combined like anisotropic filtering or stochastic model-based segmentation during the two processes.

The paper describes the main features of the method, and gives some segmentation results.

Key-Words: MRI, Segmentation, anisotropic filtering, Markov Random Field, MAP criterion.

1. INTRODUCTION

Magnetic Resonance Imaging (MRI) provides detailed images of human tissues. Particularly, it allows the observation of different brain structures such as white matter, grey matter, ventricles. In addition, data obtained from MR images can be used for detecting brain pathologies like tumors or sclerosis.

The observation of pathological regions and the measurement of tumoral response (volume, degree of necrosis, ...) have great influences on the choice and the follow up of therapies. An objective and repeatable measurement of this tumoral response is essential to appreciate the efficiency of treatments [1]. Nowadays, the volume is usually determined manually from slices but this method depends hugely on the acquisition type [2]. So, an automatic estimation of the tumoral volume is currently studied.

To this aim, the first step is obviously to segment the MR images into homogeneous regions (ideally, each region corresponds to a particular brain structure) and to localize possible tumors. This is the objective of our work.

We used images obtained from the radiology department of the Poitiers's hostipal. Different acquisition types (T1, T1-Gadolinium and T2) [3], each providing a series of slices, and different resolutions have been used. To optimize our treatment and calculating time, we decide to first separate the brain from the rest of the image in the different slices. We call this *the brain mask*. This first segmentation limits the region for a stochastic model-based unsupervised segmentation [4] of brain tissues. The choice of this segmentation method is influenced by the fact that the grey levels of brain tissues in a MRI have gaussian distributions [5].

In the second part, we present the method to obtain the brain mask from 2D-slices. In the third part, the unsupervised method for the brain tissue segmentation is detailed. We discuss the results and the future works in the last part.

2. THE BRAIN MASK

Obtaining brain contours is usually the first step of a brain segmentation process. The contour approach and the region approach are typical techniques used for the segmentation. The first one includes some standard methods such as deformable model [6] or extraction and contours tracking thanks to Laplacian operator [7]. For the second one, thresholding or regions growing [8] are some examples. In fact, several methods are often combined to improve results.

To obtain the brain mask, we use different techniques and steps inspired from [9]. First, we remove the background noise which, is supposed to be independently and identically distributed (i.i.d) and to follow the Rayleigh distribution:

$$p_n(y) = \frac{y}{\sigma^2} \exp\left(\frac{y^2}{\sigma^2}\right) \quad (1)$$

where y is the noise intensity and σ its standard deviation. The noise is eliminated by a low-thresholding (we suppose

that the first peak of the grey level histogram is due to the noise).

In a second step, a diffusion process is used to smooth the regions. Perona and Malik introduced such process [10] through the anisotropic filtering. This filter encourages intra-regions smoothing while inhibiting inter-region smoothing. The diffusion equation is done by:

$$\frac{\partial}{\partial t} I(\mathbf{s},t) = \nabla \left(c(\mathbf{s},t) \nabla I(\mathbf{s},t) \right) \tag{2}$$

where $I(\mathbf{s},t)$ is the image, $\mathbf{s} = (i,j)$, t refers to the iteration step and $c(\mathbf{s},t)$ is the diffusion function. The particular diffusion function used is defined by

$$c(\mathbf{s},t) = \exp\left(- \left| \frac{\nabla I(\mathbf{s},t)}{K} \right|^2 \right) \tag{3}$$

where K is a constant.

The images are then automatically thresholded: the threshold level is determined by fitting a Gaussian curve to the histogram of the diffused images. A connexe component labeling followed by a filling is applied to fill the possible holes. This solution is preferred to the morphologic one because it avoids the problem of choosing a kernel.

A priori localization information are used to select the finally brain mask if eyes or skulls remains.

3. UNSUPERVISED SEGMENTATION

Our purpose is now to segment the brain interior into homogeneous regions of distinct statistical behavior. Each region can be considered as a single texture and is the image of one brain structure or cerebral tumor. Moreover, a region is not supposed to be connexe. Since the number of tumors in a particular image is unknown, we can not set *a priori* the texture number. This justifies the choice of an unsupervised method.

The proposed method uses Markov Random Field (MRF) to model the discrete field containing the classification of each singular pixel i.e. the segmentation field. In MRF, the value of a pixel is statically dependent only on the value of its neighbors. This strict dependency restricts considerably the model complexity. We used a maximum *a posteriori* estimator (MAP) to estimate the realization of this hidden Markov field given the dependent observed data (the MR image).

3.1. MAP estimation

We will assume that the observed image y is a realization of a random field Y defined on a grid S of N pixels. The value of the pixel at the location s will be noted y_s. The segmentation field X is also supposed to be a random field defined on S. An element s of X takes value in $[1,\dots,M]$ where M is the texture number in the image. The conditional density function of X given Y is assumes to exist. The MAP estimation of the segmentation field of X given Y is given by:

$$\begin{aligned} \hat{x}_{MAP} &= \arg\max_x \{P(X=x|Y=y)\} \\ &\propto \arg\min_x \{-\log f(y|x) - \log f(x)\} \end{aligned} \tag{4}$$

where $f(y|x) = P(Y=y|X=x)$, $f(x) = P(X=x)$ and $P(Y=y)$ is a constant.

3.1.1. Conditional density $f(y|x)$

In [5], Geraud shows that the intensity of each particular brain structure has a gaussian distribution. A MR image, compound of M structures, can be considered as the result of a random field composed by M i.i.d gaussian processes with density functions f_i with $i = 1,\dots,M$. Each function f_i is characterized by $\theta_i = [\mu_i, \sigma_i^2]$ with μ_i the mean and σ_i the variance and defines a particular texture. We denote $\theta = [\theta_1,\dots,\theta_M]$.
The independence of the observed data leads to:

$$f(y|x) = \prod_{s\in S} \frac{1}{\sqrt{2\pi\sigma_{x_s}^2}} . \exp\left\{ \frac{1}{2} \sum_{s\in S} \frac{(y_s - \mu_{x_s})^2}{\sigma_{x_s}^2} \right\}. \tag{5}$$

So, the negative "loglikelihood" of y given x can be written as a sum of local functions of y and x:

$$-\log f(y|x) = \sum_{s\in S} l_s(y|x) \tag{6}$$

where

$$l_s(y|x) = \frac{1}{2} \left\{ \frac{(y_s - \mu_{x_s})^2}{\sigma_{x_s^2}} + \log(\sigma_{x_s}^2) + \log(2\pi) \right\}. \tag{7}$$

3.1.2. Segmentation Field Model $f(x)$

We use MRF to model the segmentation field X. In this case, the conditional distribution of a point depends on only its neighbors. In the neighborhood system, the distribution of X is a Gibbs distribution and is written [11]:

$$f(x) = \frac{1}{z} \exp\left(-U(x) \right). \tag{8}$$

where U is a potential function dependent on the neighborhood and z a normalization term, which depends on M.

However, it is quite difficult to optimize the MAP function globally. That is why we use the Iterated Conditional Mode algorithm (ICM). This algorithm maximizes the probability of the unknown field by deterministically and iterativly changing the value of pixel classification. Each change

reduces locally and so globally the estimation function (4). Although ICM is computationally efficient, it is prone to be trapped in local minima. A multiple resolution segmentation (MRS) algorithm [4] can reduce this drawback. Moreover it considerably reduces the computation time. In MRS, we first segment the image at coarse resolution n, then we use the segmented image as an initialization at the $(n-1)$ resolution and so on until the finest resolution.

For a fixed number M of classes, the MAP estimation of the segmentation field is computable using the multiscale ICM segmentation. However, since the normalization term z depends on the unknown texture number M, the MAP estimation is not tractable from one number of class to another. To overcome this difficulty, we approximate the Gibbs distribution by a multinomial distribution at the coarsest resolution in the MRS algorithm and we apply the following procedure.

3.2. Multinomial distribution

The approximation of Gibbs distribution by a multinomial distribution is only made at the first stage of the MRS algorithm in order to estimate the final number M of class and the value of the parameters $\theta = [\theta_1, \dots, \theta_M]$. The approach is to divide the image in blocks of equal size (this defines a block grid $S^{(n)}$). The neighboring information are ignored in supposing that blocks are randomly reordered. Moreover, we suppose that each block contains one single texture. We denote $A_k \subset S^{(n)}$ a set of blocks which have a texture of type k for $k = 1, \dots, M$ and W_k the number of pixels in the set A_k with $W = \sum_{k=1}^{M} W_k$. The probability ρ_k, estimated by $\hat{\rho_k} = \frac{W_k}{W}$, of a particular texture is defined by the multinomial distribution. We denote $\rho = [\rho_1, \dots, \rho_M]$.

Finally, our model is defined by the partitioning set $\{A_k\}_{k=1}^{M}$, the parameters of textures $\theta_\rho = (\theta, \rho)$ and the number M of classes. Bouman shows in [4] that the conditional joint distribution of y and the partitioning set $\{A_k\}_{k=1}^{M}$ given θ_ρ is:

$$p_{\theta_\rho}(y, A_1, \dots, A_M) = \prod_{k=1}^{M} \exp\{-L(\xi_{A_k}, \theta_k) + W_k \log \rho_k\} \quad (9)$$

where

$$-L(\xi_{A_k}, \theta_k) = \sum_{s \in A_k} l_s(y|k). \quad (10)$$

3.3. Information Criteria

To estimate the set of model parameters we use an information criterion. Such criteria are based on the computation of the model likelihood while penalizing them through an additional term depending on the number of free parameters. In [4], Akaike criterion was used but it has been proved that this criterion is not consistent. Here, we propose to use the ϕ_β criterion [12]

$$\phi_\beta = -2 \log p_{\theta_\rho}(y) + C_{\phi_\beta}(Q).k \quad (11)$$

where

- $p_{\theta_\rho}(y)$ is the conditional distribution of y considering the model θ_ρ
- $k = 3M - 1$ is the number of free parameters
- $C_{\phi_\beta}(Q) = Q^\beta \log(\log(Q))$ with $\beta = \frac{\log(\log(Q))}{\log(Q)}$ according to [13].
- and Q is the number of observed data.

However the use of $p_{\theta_\rho}(y)$ is complex. Bouman proposes to replace it by:

$$-2 \log p_{\theta_\rho}(y, A_1, \dots, A_M) + C_{\phi_\beta}(Q).k \quad (12)$$

The texture number M, the partitioning set $\{A_k\}_{k=1}^{M}$ and the parameters (θ_i, ρ_i) of each texture will be then estimated using three procedures each of which strictly reduces the criterion of the formula (12). Each of these procedures may be thought as minimizing with respect to one of M, (θ, ρ) or $\{A_k\}_{k=1}^{M}$ while fixing the remaining two quantities.

4. RESULTS AND FUTURE WORKS

The images were acquired axially on GE 1.5 Tesla MRI scanner. The data consist of slices with 256 x 256 (for the healthy slices) or 512 x 512 (for the unhealthy one) pixels per slices.

The figure 1 shows segmentation result of a healthy brain. As we can see, the main structures were fund (white matter, grey matter and ventricles). Meanwhile, we observe that a same label can be assigned to different brain structures (white matter and the external parts of ventricles for example) if the mean grey level of structures are very close.
The figure 2 shows the result obtained with unhealthy brain. The main observation is that the tumor is well localized (the brightest region on figure 2.2). Next to this region, the ecchymosis caused by the tumor is detected too. The other brain regions are coherent towards the grey levels of the image.

Expert studies show that such results are clinically acceptable. Their exploitation for the volume measurement is possible.

In future work, this unsupervised segmentation method will be extended in three dimensions. Indeed, the third dimension should bring additional information and allow better segmentation results.

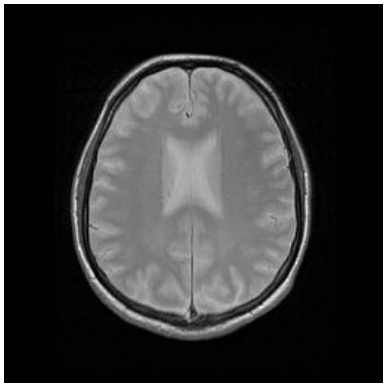

(1.1) original slice

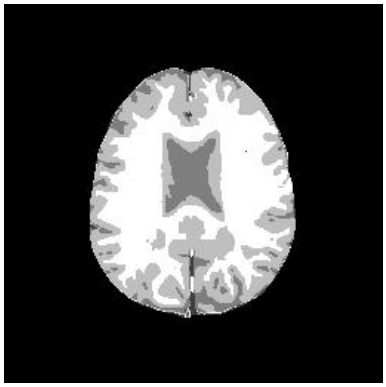

(1.2) segmented slice

Fig. 1. T2 brain slice without tumor

(2.1) original slice

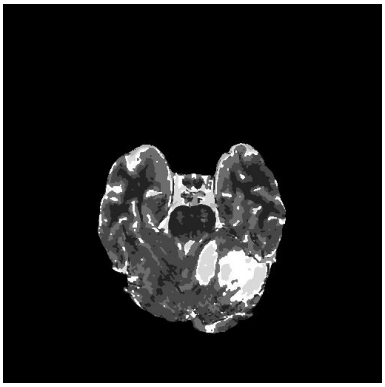

(2.2) segmented slice

Fig. 2. T2 brain slice with tumor

5. REFERENCES

[1] D'Amico A.V., Chang E., Garnick M., Kantoff P., Jiroutek M., and Tempany C.M. Assessment of prostate cancer volume using endorectal coil resonance imaging: a new predictor of tumor response to neoadjuvant androgen therapy. *Urology*, 51:287–292, 1998.

[2] Dubois D.F., Prestidge B.R., Hotshkiss L.A., Prete J.J., and Bice W.S. Intraobserver and interobserver variability of mr imaging and ct derived prostate volumes after transperineal intersticial permanent prostate brachytherapy. *Radiology*, 207(785–789), 1998.

[3] Cueno C.A., Doyon D., and Halimi P. *Anatomie IRM de la tête*. Masson, 1989.

[4] Bouman C. Multiple resolution segmentation of textured images. *IEEE Trans. on Pattern Analysis and Machine Intelligence*, 13(2):99–113, Feb 1991.

[5] Geraud T. *Segmentation des structures internes du cerveau en imagerie par résonance magnétique tridimentionnelle*. PhD thesis, Ecole Nat. Sup. des Télécommunication, 1998.

[6] McInerney T. and Terzopoulos D. Deformable models in medical image analysis: A survey. *Medical Image Analysis*, 1(2):91–108, 1996.

[7] Raman S., Sarkar S., and Boyer K. Tissue boundary refiment in magnetic resonance images using contour-based scale space matching. *IEEE Trans. on Medical Imaging*, 10(2):190–221, 1991.

[8] Garza-Zinich, Meer P., and Medina V. Robust retrieval of 3d structures for magnetic resonance images. *Proc of Int. Conf. on Pattern Recog*, 3:391–395, 1995.

[9] Stella M. and Blair T. Mackievich. Fully automatic segmentation of brain in mri. *IEEE Trans. on Medical Imaging*, 17(1):98–107, 1998.

[10] Perona P. and Malik J. Scale-space and edge detection using anisotropic diffusion. *IEEE Trans. Pattern and Machine Intell.*, 12:662–667, July 1990.

[11] S. Geman and D. Geman. Stochastic relaxation, gibbs distribution, and the bayesian restauration of images. *IEEE Trans. Pattern Anal. Machine Intell.*, PAMI-6, Nov. 1984.

[12] A. El Matouat and M. Hallin. Order selection, stochastic complexity and kull back-leiber information. *P.M. Robinson and M. Rosenblatt editors, Time series analysis, in memory of E.J. Hannan*, 2:291–299, 1996.

[13] O. Alata and C. Olivier. Order selection of 2-D AR model using a lattice representation and information criteria for texture analysis. *to be published in EUSIPCO*, 2000.